ARTICLE NO. 79-4097

Calculation of Rotor Impedance for Articulated-Rotor Helicopters in Forward Flight

Kanichiro Kato* and Takashi Yamane†
University of Tokyo, Tokyo, Japan

A procedure is presented to calculate the loads transferred from an articulated flexible rotor to the fuselage when the hub is forced to oscillate sinusoidally. Blade motions are determined from a set of linear algebraic equations derived from equations of motion with periodic coefficients. The aerodynamic loads are based on two-dimensional quasisteady strip theory and the effect of preceding and returning wakes as well as the reversed flow are neglected. Sample calculations indicate that: 1) the major components of impedances with hub-forcing frequency predominate over those with interharmonic coupling frequencies; 2) the former impedances do not depend on the blade azimuth angle relative to the hub excitation phase; and 3) the former impedances are similar to those obtained in hovering flight.

I. Introduction

WHEN a rotor hub is forced to oscillate sinusoidally, the following linear relations can be defined between the hub motions and the hub loads transferred from the rotor to the fuselage.

$$\begin{Bmatrix} \Delta H_s \\ \Delta Y_s \\ \Delta T_s \\ \Delta M_{xs} \\ \Delta M_{ys} \\ \Delta M_{zs} \end{Bmatrix} = \begin{bmatrix} \\ \\ & Z_R & \\ \\ \\ \end{bmatrix} \begin{Bmatrix} -\Delta U \\ \Delta V \\ -\Delta W \\ -\Delta P \\ \Delta Q \\ -\Delta R \end{Bmatrix} \tag{1}$$

where Δ denotes small changes from a trim condition and $-\Delta U = e^{i\omega t}$, etc. Referring to Fig. 1, (U, V, W, P, Q, R) are the velocities and the angular velocities of a hub and $(H_s, Y_s, T_s, M_{xs}, M_{ys}, M_{zs})$ are the forces and the moments, respectively, measured in the shaft frame X_s, Y_s, Z_s fixed to the fuselage. In this paper, the matrix Z_R in Eq. (1) is called the rotor impedance matrix; each element in Z_R expresses an impedance corresponding to a perturbed hub motion and a hub load variation. In forward flight, the blade equations have periodic coefficients, causing the impedance Z_R to be a function not only of the hub frequency ω but also of the reference blade azimuth angle.

The authors proposed in Ref. 1 a procedure of the impedance calculation for hovering articulated rotors and showed how the rotor impedances are influenced by elastic, inertial, and aerodynamic loads for varying hub-forcing frequencies.

In hover, impedance calculations are essentially frequency-response calculations, because only the loads having the forcing frequency are transferred to the fuselage if the number of blades is three or more. On the other hand, the response loads transferred to the fuselage in forward flight have not only the forcing frequency ω but also the interharmonic coupling frequencies $\omega \pm kN\Omega$ $(k=1,2,\ldots,\infty)$, where N and Ω denote the number of blades and the rotor angular velocity, respectively. In addition, the blade azimuth angle relative to hub excitation phase is a new independent parameter.

This paper formulates a procedure to calculate the rotor impedances in forward flight and gives results of a sample calculation for an articulated rotor that has the same properties as one used in Ref. 1. Aerodynamic loads are assumed to be based on quasisteady strip theory and the reversed flow is neglected. Another assumption is that the Fourier coefficients in blade motion representations can be truncated at a finite number of harmonics; the higher order harmonics are neglected in the analysis.

References 2 and 3 conduct hingeless rotor response analysis, and a Generalized Harmonic Balance Method is used when solving the blade and the hub-load equations. Virtually, the similar approaches are taken in this paper. However, this paper conducts all the calculations in the complex domain, simplifying the formulations to a great extent. Also, this paper differs from Refs. 2 and 3 in the following respects. They consider only flap deflections and the numerical results are given in terms of steady-state thrust and moment derivatives for steady ($\omega = 0$) shaft incidence as well as blade

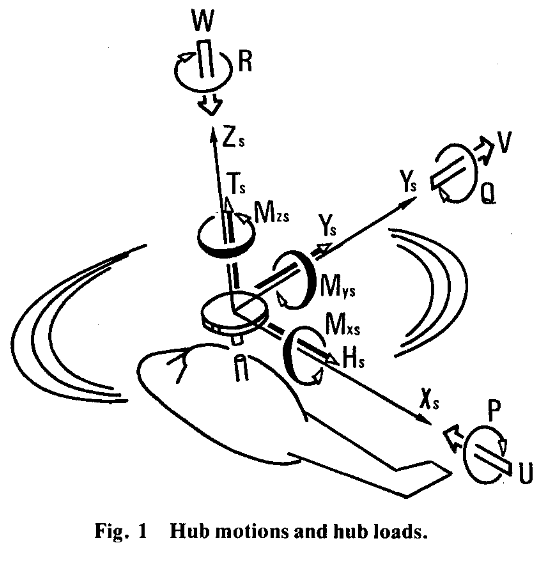

Fig. 1 Hub motions and hub loads.

Received May 23, 1978; revision received Nov. 27, 1978.

Index categories: Helicopters; Vibration; Aeroelasticity and Hydroelasticity.

*Associate Professor, Department of Aeronautics.
†Graduate Student, Department of Aeronautics.

pitch controls. This paper covers flap-lag-torsion coupled analysis and the results are given in terms of hub impedances; that is, forces and moments for harmonic hub excitations with arbitrary frequencies.

II. Blade Equations of Motion

When the hub is forced to oscillate, blade equations of motion can be summarized as follows. Referring to Fig. 2, the rotating hub frame X_R, Y_R, Z_R rotates about the shaft axis Z_S with rotor rotational speed Ω. Blade displacements are described in the rotating hub frame, and ϕ, w, and v denote torsional, flapwise, and chordwise displacement in X_R, Y_R, Z_R frame. These displacements can be approximately expressed in terms of coupled natural mode shapes $\bar{\phi}_j$, $\bar{w}_j$, and $\bar{v}_j$, as follows.

$$\phi=\sum_{j=1}^{\ell}\bar{\phi}_j q_j \qquad \omega=\sum_{j=1}^{\ell}\bar{w}_j q_j \qquad v=\sum_{j=1}^{\ell}\bar{v}_j q_j \tag{2}$$

where q_j is the generalized coordinate of the jth mode. Then, the blade equations of motion can be given as:

$$m_j\ddot{q}_j+m_j\omega_j^2 q_j=Q_j \qquad (j=1,2,\ldots,\ell) \tag{3}$$

where m_j, ω_j, and Q_j are the generalized mass, the natural frequency, and the generalized force of the jth coupled natural mode, respectively.

In the particular case where the chordwise center of gravity location and the elastic axis coincide with the feathering axis, Q_j has the following expression:

$$\begin{aligned}Q_j=\int_0^R [\{m_x+M-mk^2(\ddot{\theta}+\Omega^2\theta+2\Omega\theta\dot{v}')\}\bar{\phi}_j\\ +\{f_z+L-mg-2m\Omega w_0'\dot{v}\}\bar{w}_j\\ +\{f_y-D-D_i-2m\Omega\dot{u}\}\bar{v}_j]\mathrm{d}r\end{aligned} \tag{4}$$

where $\theta=\theta_0-A_1\cos\psi-B_1\sin\psi$. m_x, f_z, and f_y denote inertial load contributions to the torsional moment, forces along Z_R- and Y_R-axis per unit span, respectively while M, L, and $D+D_i$ denote the aerodynamic load contributions in a similar manner. R, m, and k are the blade radius, the mass per unit span, and the polar radius of gyration in torsion, respectively. u denotes the blade radial displacement along the X_R-axis which causes an in-plane Coriolis force and is approximated as:

$$u=\sum_{j=1}^{\ell}\bar{u}_j q_j \qquad \bar{u}_j\cong-\int_0^r w_0'\bar{w}_j'\mathrm{d}r \tag{5}$$

where w_0 is the time-averaged flapwise displacement.

The detail derivation of the blade perturbation equations for the case of hovering flight are given in Ref. 1. Two modifications are conducted for the application to forward flight. First, the expressions for the relative velocity vector of the airflow are changed so that the forward-flight velocity vector can be included. Referring to Fig. 2 and using the same notations and coordinate systems as in Ref. 1, the relative air velocities U_a and H_a [Eq. (22) in Ref. 1] are modified to the following form:

$$\begin{aligned}U_a&=r(\Omega-\dot{R})+\dot{v}+(U\sin\psi+V\cos\psi)+v'U\cos\psi\\ H_a&=-v_s-\dot{w}+W+r(P\sin\psi+Q\cos\psi)-w'U\cos\psi\end{aligned} \tag{6}$$

where U and W are the hub velocities in the $-X_S$ and $-Z_S$ (shaft) directions, as shown in Fig. 1, and are resolved into

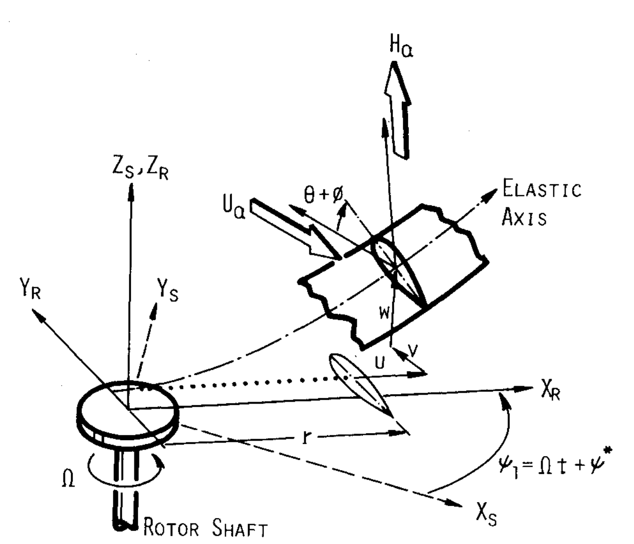

Fig. 2 Variables for a blade motion.

trim values and perturbed values as:

$$U=U_0+\Delta U \qquad V=\Delta V \qquad W=W_0+\Delta W \tag{7}$$

Secondly, the blade tension T along the X_R-axis is modified so that the effect of radial Coriolis force due to lead-lag motion be included; that is,

$$T=\int_r^R (r\Omega^2+2\Omega\dot{v})m\mathrm{d}r \tag{8}$$

Though this results in additional terms in generalized forces, only the term $-2m\Omega w_0'\dot{v}$ from the flap bending equation is retained; the other terms from torsional and lead-lag bending equations can be neglected as higher order terms.

III. Steady-State Solution of Blade Motion

Equation (3) gives a set of simultaneous differential equations concerning $q_j(j=1,2,\ldots,\ell)$, and $\Delta U=\Delta V=\ldots=\Delta R=0$ results in a solution $\bar{q}_j$, which corresponds to a trim flight condition. When the hub motion

$$-\Delta U,\ \Delta V,\ -\Delta W,\ -\Delta P,\ \Delta Q,^{\prime}\text{ or }-\Delta R=e^{i\omega t} \tag{9}$$

is superimposed on the trim condition, an additional blade motion will appear. Now, if the hub motion is assumed to be small, the incremental blade motion can be described by a small perturbation Δq_j from the trim value $\bar{q}_j$. If the perturbation generalized coordinate vector, Δq, is defined as:

$$\Delta q=[\Delta q_1,\Delta q_2,\ldots,\Delta q_\ell]^T \tag{10}$$

then Δq can be shown to be described by a second-order linear vector differential equation.

For clarity, we first consider the situation in hovering flight. In this case Δq can be obtained by the following differential equation with constant coefficients:

$$A_\Delta\ddot{q}+B_\Delta\dot{q}+C_\Delta q=x_{-1}e^{i(\omega t-\psi)}+x_0e^{i\omega t}+x_1e^{i(\omega t+\psi)} \tag{11}$$

where A, B, and C are constant real matrices. x_{-1}, x_0, and x_1 are amplitude vectors of forcing terms due to a hub motion and ψ and ω are the azimuth angle of each blade and hub forcing frequency, respectively. The steady-state solution can be expressed as a sum of motions having three frequencies:

$$\Delta q=\hat{q}_{-1}e^{i(\omega t-\psi)}+\hat{q}_0e^{i\omega t}+\hat{q}_1e^{i(\omega t+\psi)} \tag{12}$$

The hub loads obtained from this motion should have frequency components of ω, $\omega \pm \Omega$, and $\omega \pm 2\Omega$ when they are transformed to the fuselage shaft frame. However, if the number of blades N is three or more, only the loads having the frequency ω are transferred to the fuselage in the case of hovering, since the $\omega \pm \Omega$ and $\omega \pm 2\Omega$ components cancel each other after the multiblade summation.

In forward flight, A, B, and C in Eq. (11) become time-varying periodic matrices, and higher-order harmonics of ψ appear in the right-hand side of Eq. (11). When the two-dimensional quasisteady strip theory is used, there appear harmonics of ψ up to the third and Eq. (11) is modified to the following form, where A_n, B_n, C_n, and x_m are all complex:

$$\sum_{n=-3}^{3} [(A_n e^{in\psi})\Delta\ddot{q} + (B_n e^{in\psi})\Delta\dot{q} + (C_n e^{in\psi})\Delta q] = \sum_{m=-3}^{3} x_m e^{i(\omega t + m\psi)} \tag{13}$$

Let us assume the solution of Eq. (13) as:

$$\Delta q = \sum_{k=-\infty}^{\infty} \hat{q}_k e^{i(\omega t + k\psi)} \tag{14}$$

where $\hat{q}_k$ is a complex, constant vector. If Eq. (14) is substituted into Eq. (13) and the same harmonic components in either side are equated, we have an infinite number of simultaneous equations concerning $\hat{q}_k$ $(k = -\infty \ldots +\infty)$. If the amplitudes $\hat{q}_k$ are truncated at a finite number of harmonics, the following equations will be obtained, where h is an integer and the maximum harmonic number of ψ contained in the following:

$$\begin{bmatrix} R_{-h,-h} & \cdots & R_{-h,-h+3} & 0 & \cdots & 0 \\ \vdots & \ddots & & \ddots & \ddots & \vdots \\ R_{-h+3,-h} & & \ddots & & \ddots & 0 \\ 0 & \ddots & & \ddots & & R_{h-3,h} \\ \vdots & \ddots & \ddots & & \ddots & \vdots \\ 0 & \cdots & 0 & R_{h,h-3} & \cdots & R_{h,h} \end{bmatrix} \begin{Bmatrix} \hat{q}_{-h} \\ \vdots \\ \vdots \\ \vdots \\ \vdots \\ \hat{q}_h \end{Bmatrix} = \begin{Bmatrix} 0 \\ \vdots \\ 0 \\ x_{-3} \\ \vdots \\ x_3 \\ 0 \\ \vdots \\ 0 \end{Bmatrix} \tag{15}$$

where

$$R_{jk} = -(\omega + k\Omega)^2 A_{j-k} + \sqrt{-1}(\omega + k\Omega) B_{j-k} + C_{j-k} \tag{16}$$

The derivation of Eqs. (15) and (16) will be found in the Appendix. By solving Eq. (15), constant amplitudes of $2h+1$ generalized coordinates, $\hat{q}_k$, can be determined, and the blade motion can be approximated by:

$$\Delta q = \sum_{k=-h}^{h} \hat{q}_k e^{i(\omega t + k\psi)} \tag{17}$$

The method for solution in Refs. 2 and 3 is to express a generalized coordinate q_j in the following form:

$$q_j - \bar{q}_j = \{a_{j0} + \sum_{n=1}^{N} [a_{jn}\cos n\psi + b_{jn}\sin n\psi]\} e^{i\omega t}$$

This approach necessitates the use of cumbersome matrix operations. If the blade motion is described as given by Eq. (17) and if all the computations are directly done in complex domain, the analyses can be greatly simplified; the main effort is only to define A_n, B_n, and C_n $(n = -3, \ldots, 3)$ in a computer storage. This easily enables the inclusion of fully-coupled blade dynamics in the impedance calculations.

IV. Impedance Calculations

Let ψ_1 denote the blade azimuth angle and let vectors ΔF_1 and ΔM_1 denote the variations in hub forces and moments, respectively, where the suffix $(\ )_1$ is used to give emphasis on blade 1. The augmented vector $[\Delta F_1^T, \Delta M_1^T]^T$ can be expressed in the following form in the rotating hub frame:

$$\begin{Bmatrix} \Delta F_1 \\ \Delta M_1 \end{Bmatrix}_{\text{rot}} = d(\psi_1) e^{i\omega t} + E(\psi_1)\Delta\ddot{q} + F(\psi_1)\Delta\dot{q} + G(\psi_1)\Delta q \tag{18}$$

where d denotes a complex vector which gives the loads of the perfectly rigid blade and E, F, and G denote complex matrices which account for the effects of the blade displacement, d through G are all functions of the azimuth angle of blade 1, ψ_1, and each has harmonics in ψ_1 up to the third. Therefore, the substitution of Eq. (17) into Eq. (18) results in the following form:

$$\begin{Bmatrix} \Delta F_1 \\ \Delta M_1 \end{Bmatrix}_{\text{rot}} = \sum_{n=-3}^{3} s_n e^{i(\omega t + n\psi_1)} + \sum_{n=-3}^{3} \sum_{k=-h}^{h} T_{nk} \hat{q}_k e^{i(\omega t + k\psi_1 + n\psi_1)} \tag{19}$$

where s_n and T_{nk} denote a constant vector and a constant matrix, respectively.

The hub loads can be transformed to the shaft frame fixed to the fuselage as follows:

$$\begin{Bmatrix} \Delta F_1 \\ \Delta M_1 \end{Bmatrix}_{\text{fus}} = \left[\begin{array}{c|c} \boldsymbol{\Psi} & 0 \\ \hline 0 & \boldsymbol{\Psi} \end{array}\right] \begin{Bmatrix} \Delta F_1 \\ \Delta M_1 \end{Bmatrix}_{\text{rot}} \tag{20}$$

where

$$\boldsymbol{\Psi} = \begin{bmatrix} \cos\psi_1 & -\sin\psi_1 & 0 \\ \sin\psi_1 & \cos\psi_1 & 0 \\ 0 & 0 & 1 \end{bmatrix} \tag{21}$$

This transformation increases the highest harmonic number of ψ_1 by one and the fuselage hub loads can be expressed in the following form:

$$\begin{Bmatrix} \Delta F_1 \\ \Delta M_1 \end{Bmatrix}_{\text{fus}} \equiv \sum_{\nu=-h-4}^{h+4} z_\nu e^{i(\omega t + \nu\psi_1)} = \sum_{\nu=-4}^{4} y_\nu e^{i(\omega t + \nu\psi_1)} + \sum_{\nu=-h-4}^{h+4} \sum_{k=-h}^{h} S_{\nu k} \hat{q}_k e^{i(\omega t + \nu\psi_1)} \tag{22}$$

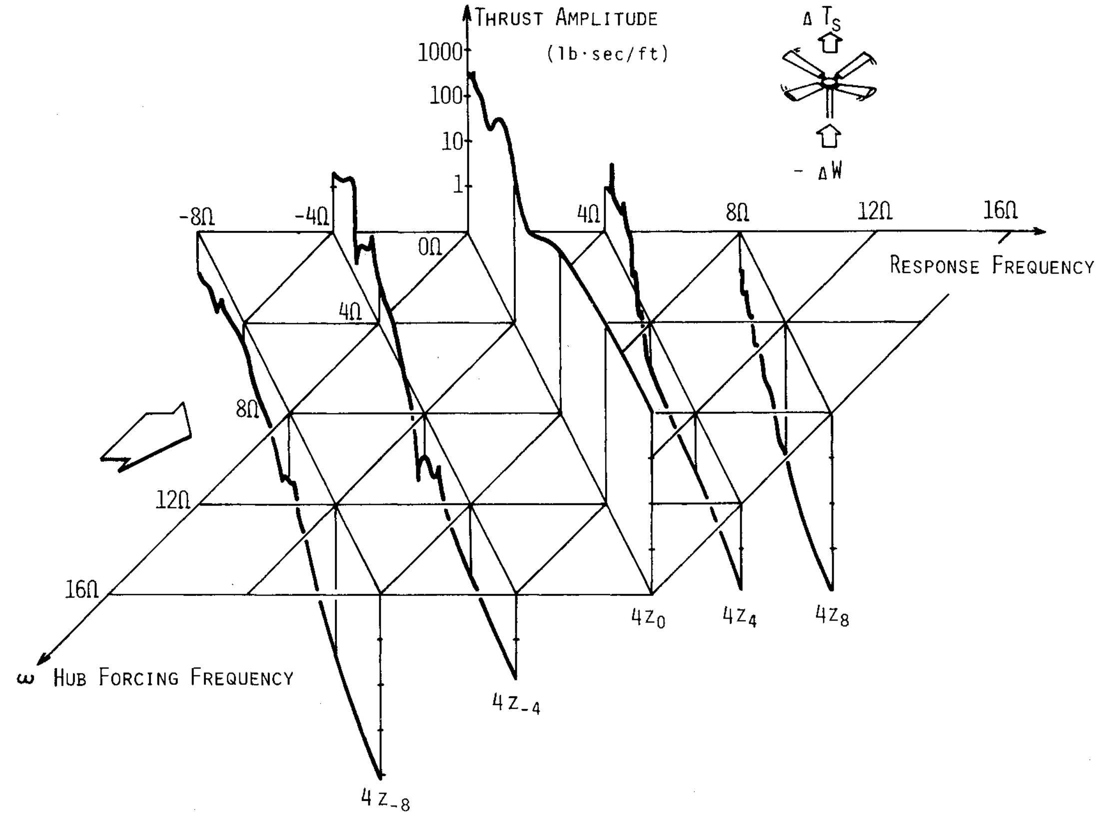

Fig. 3 Perspective view of thrust response vs hub motion.

where z_ν, a vector having six elements, denotes the νth harmonic component of the hub loads transferred to the fuselage. Since the Fourier coefficients have been truncated at the hth harmonic in the blade motion representation [refer to Eqs. (15) and (17)], the fuselage loads should also be truncated at the hth harmonic. A manipulation similar to that used in the Appendix results in the following relation:

$$\begin{Bmatrix} z_{-h} \\ \vdots \\ \vdots \\ \vdots \\ z_h \end{Bmatrix} = \begin{Bmatrix} 0 \\ \vdots \\ 0 \\ y_{-4} \\ \vdots \\ y_4 \\ 0 \\ \vdots \\ 0 \end{Bmatrix} + \begin{bmatrix} S_{-h,-h} & \cdots & S_{-h,-h+4} & 0 & \cdots & 0 \\ \vdots & & & \ddots & & 0 \\ S_{-h+4,-h} & & & & \ddots & \\ 0 & \ddots & & & & S_{h-4,h} \\ \vdots & & & & & \vdots \\ 0 & \cdots & 0 & S_{h,h-4} & \cdots & S_{h,h} \end{bmatrix} \begin{Bmatrix} \hat{q}_{-h} \\ \vdots \\ \vdots \\ \hat{q}_h \end{Bmatrix} \tag{23}$$

The total hub loads consist of the combined effects of all N blades. Let the azimuth angle of each blade be denoted by ψ_j $(j=1,\ldots,N)$. Using the multiblade summation formula:

$$\sum_{j=1}^{N} e^{i\nu\psi_j} = \begin{cases} Ne^{i\nu\psi_1} & : \nu/N=\text{integer} \\ 0 & : \text{otherwise} \end{cases} \tag{24}$$

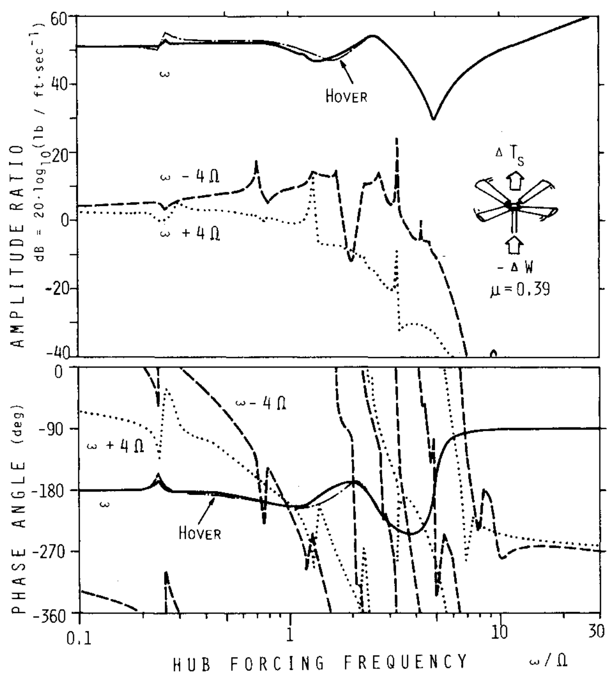

Fig. 4 Thrust variation vs hub plunging velocity.

the following can be obtained:

$$\sum_{j=1}^{N} \begin{Bmatrix} \Delta F_j \\ \Delta M_j \end{Bmatrix}_{\text{fus}} = N \sum_{|k| \le h/N} z_{k\cdot N} e^{i(\omega t + kN\psi_1)}$$

$$= N \sum_{|k| \le h/N} z_{k\cdot N} e^{i(\omega t + kN(\Omega t + \psi^*))} \tag{25}$$

where ψ^* is the initial azimuth angle of blade 1; that is,

$$\psi_I(t) = \Omega t + \psi^* \tag{26}$$

where t is selected so that the hub motion is taken as $e^{i\omega t}$.

Two important characteristics appear in Eq. (25). First, the term with $k=0$, which will be shown later to be the major part of the impedance, does not depend on ψ^* or the relative phase between the hub-forcing motion and the rotor-rotating motion. Second, the amplitude level of those terms with $k \neq 0$ are not influenced by ψ^*, since the effect of ψ^* is only to introduce a phase shift of $kN\psi^*$ radians.

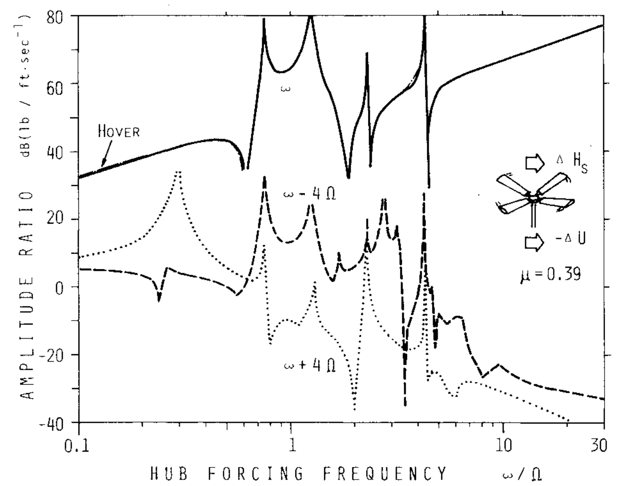

Fig. 5 *H*-force variation vs hub fore and aft velocity.

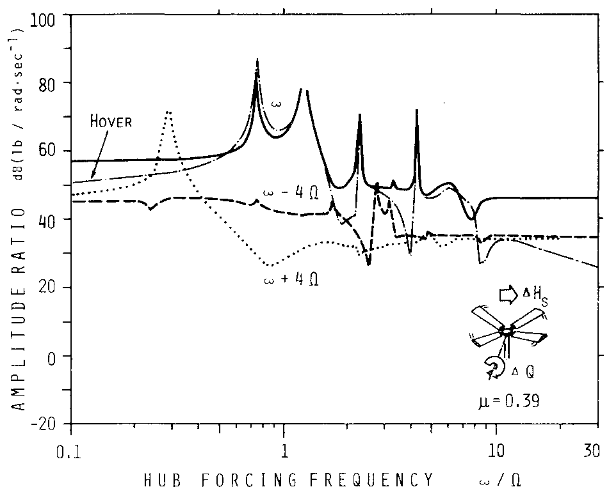

Fig. 6 *H*-force variation vs hub pitching rate.

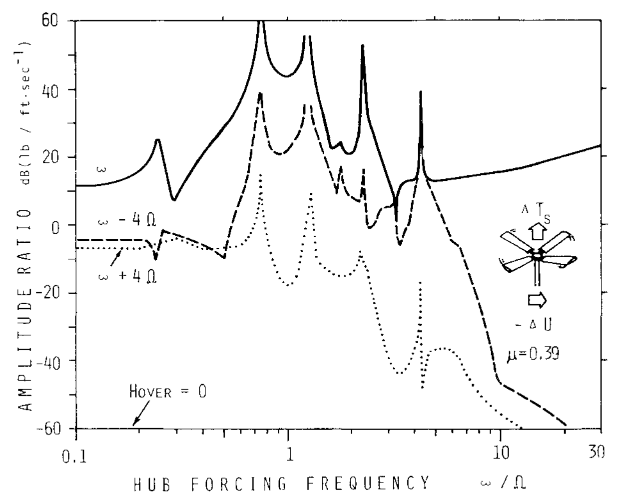

Fig. 7 Thrust variation vs hub fore and aft velocity.

V. Sample Calculations and Discussion

Numerical calculations were conducted for an articulated rotor of 28 ft radius and 1.366 ft chord. All of the rotor dimensions are the same as that used in Ref. 1, where the chordwise c.g. location and the elastic axis coincide with the feathering axis. The number of blades N is four.

Rotor operating conditions are as follows. All values with suffix $(\ )_s$ refer to the shaft frame X_s, Y_s, Z_s.

Thrust coefficient	C_{T_s}	=	0.0044
Advance ratio	μ_s	=	0.39
Inflow ratio	λ_s	=	−0.038
Shaft angle of attack	α_s	=	−0.079 rad
Collective pitch angle	θ_0	=	0.150 rad
Steady coning angle	w_0'	=	0.085 rad
Longitudinal cyclic control	B_I	=	0.103 rad
Lateral cyclic control	A_I	=	0
Rotor angular velocity	Ω	=	23.2 rad/s

The inflow ratio λ_s is assumed to be uniform over the rotor disk and was determined so that the Glauert formula holds between μ_s, λ_s, α_s, and C_{T_s}.

In generalized force calculations, uncoupled mode shapes were assumed. This presumes that the blade has no twist and zero collective pitch. However, the collective pitch angle θ_0 in Eq. (4) and the steady coning w_0' in Eq. (5) are assumed to be 0.150 and 0.085 rad, respectively, as was done in Ref. 1. This was done intentionally to include and evaluate the effects of the in-plane Coriolis force.

To determine the blade motion, five uncoupled modes were used ($\ell=5$); the highest harmonic number assumed for Δq is 5 ($h=5$). Correspondingly, $|k| \leq h/N$ reduces to $k=0, \pm 1$ in Eq. (25).

Figure 3 shows a perspective view of the numerical results for the thrust variation when the hub is forced to oscillate vertically by $-\Delta W = e^{i\omega t}$. For the forcing frequency ω, the response loads transferred to the fuselage have a frequency spectrum at ω (denoted by $4z_0$), $\omega \pm 4\Omega$ ($4z_{\pm 4}$), and $\omega \pm 8\Omega$ ($4z_{\pm 8}$), . . . in the case of a four-bladed rotor. It should be noted, however, that the z_8 and z_{-8} curves (which are really qualitative pictures added for illustrative purposes) must be rejected to the $|k| \leq h/N$ assumption. An abscissa and ordinate of the horizontal plane of Fig. 3 are the input and response frequencies, while the vertical axis corresponds to the amplitude level of thrust variations.

Figure 4 shows those response curves of Fig. 3 when viewed along the direction of the arrow shown. The thrust variation with forcing frequency, shown by a solid line, predominates over the responses with interharmonic coupling frequencies of $\omega \pm 4\Omega$, which are shown by dotted and broken lines. The response with forcing frequency is hereafter called the major impedance.

A chained line in Fig. 4 is the impedance obtained for hovering flight.[1] It should be noted that the major impedance is pretty close to hover impedance.

Figure 4 also shows the phase angle characteristics of thrust vs vertical velocity impedance.

Similarly, Fig. 5 shows the *H*-force variation due to fore and aft hub motion, $-\Delta U = e^{i\omega t}$. The response amplitudes having frequencies ω and $\omega \pm 4\Omega$ are shown. As was the case in Fig. 4, the major impedance (solid line) predominates over the other impedances due to interharmonic coupling (dotted and broken line) and agrees quite well with the hover impedance (chained line). Amplitude divergence at lag resonance frequencies occurs since lag damper is not assumed in this analysis.

$$
\left[\begin{array}{ccccccccccccccccc}
{-5,-8} & {-5,-7} & {-5,-6} & {-5,-5} & {-5,-4} & {-5,-3} & {-5,-2} & & & & & & & & & & \\
 & {-4,-7} & {-4,-6} & {-4,-5} & {-4,-4} & {-4,-3} & {-4,-2} & {-4,-1} & & & & & & & & & \\
 & & {-3,-6} & {-3,-5} & {-3,-4} & {-3,-3} & {-3,-2} & {-3,-1} & {-3,0} & & & & & & & & \\
 & & & {-2,-5} & {-2,-4} & {-2,-3} & {-2,-2} & {-2,-1} & {-2,0} & {-2,1} & & & & & & & \\
 & & & & {-1,-4} & {-1,-3} & {-1,-2} & {-1,-1} & {-1,0} & {-1,1} & {-1,2} & & & & & & \\
 & & & & & {0,-3} & {0,-2} & {0,-1} & {0,0} & {0,1} & {0,2} & {0,3} & & & & & \\
 & & & & & & {1,-2} & {1,-1} & {1,0} & {1,1} & {1,2} & {1,3} & {1,4} & & & & \\
 & & & & & & & {2,-1} & {2,0} & {2,1} & {2,2} & {2,3} & {2,4} & {2,5} & & & \\
 & & & & & & & & {3,0} & {3,1} & {3,2} & {3,3} & {3,4} & {3,5} & {3,6} & & \\
 & & & & & & & & & {4,1} & {4,2} & {4,3} & {4,4} & {4,5} & {4,6} & {4,7} & \\
 & & & & & & & & & & {5,2} & {5,3} & {5,4} & {5,5} & {5,6} & {5,7} & {5,8}
\end{array}\right]
\begin{bmatrix} \hat{q}_{-8} \\ \hat{q}_{-7} \\ \hat{q}_{-6} \\ \hat{q}_{-5} \\ \hat{q}_{-4} \\ \hat{q}_{-3} \\ \hat{q}_{-2} \\ \hat{q}_{-1} \\ \hat{q}_{0} \\ \hat{q}_{1} \\ \hat{q}_{2} \\ \hat{q}_{3} \\ \hat{q}_{4} \\ \hat{q}_{5} \\ \hat{q}_{6} \\ \hat{q}_{7} \\ \hat{q}_{8} \end{bmatrix}
=
\begin{bmatrix} 0 \\ 0 \\ x_{-3} \\ x_{-2} \\ x_{-1} \\ x_{0} \\ x_{1} \\ x_{2} \\ x_{3} \\ 0 \\ 0 \end{bmatrix}
$$

Fig. 8 Numerical scheme for solving blade equations of motion.

Figure 6 shows the H-force variation due to hub pitching, $\Delta Q = e^{i\omega t}$. In this case, the major impedance differs from the hover impedance. This is attributed to the inertial force due to hub pitching with nonzero shaftwise flight velocity. In forward flight, the hub generally has a translational velocity V and this causes an acceleration $\omega \times V$ in the shaft axis system, where ω is a hub angular velocity, resulting in the inertial loads which did not appear in hover. (In usual stability derivative calculations, these loads are not included; the whole inertial loads cancel each other because the origin of the body-fixed frame is taken at the center of gravity of the helicopter.)

Figure 7 shows the thrust variation due to fore and aft hub motion, $-\Delta U = e^{i\omega t}$, in forward flight. Based on the present linearized theory, this impedance is zero in hover. This is an example where an impedance is not similar in hover and in forward flight. However, the amplitude level of this impedance is pretty low when compared with $-\Delta T_s/\Delta W$ and $-\Delta H_s/\Delta U$ of Figs. 4 and 5. Also, several amplitude peaks of $-\Delta T_s/\Delta U$ occur at lag natural frequencies and can be suppressed by lag dampers in actual articulated rotors. Therefore, it still can be said that $-\Delta T_s/\Delta U$ is similar in hover and in forward flight in the sense of being small quantity.

VI. Concluding Remarks

The significant results of the sample calculations are that the major impedances with forcing frequency: 1) predominate over the other impedances due to interharmonic coupling; 2) do not depend on the blade azimuth angle relative to the hub excitation phase; and 3) resemble those corresponding impedances obtained in hover. These results may suggest some of the typical characteristics of the rotor impedances, although the results may be limited due to the assumptions and numerical values used in the analysis.

The first conclusion is the extention of the similar proposition known in the field of the harmonic airloading of the helicopter rotor.[4] A resembling fact is reported in Ref. 5, where the flapping motions at high advance ratio are discussed in terms of multiblade coordinate. It is shown there that the omission of periodic terms has only a moderate effect on the low-frequency mode. This paper provides numerical results asserting similar supposition to the loads due the hub harmonic excitations with arbitrary frequencies.

The second conclusion will aid to simplify vibration analysis. Hitherto, rotor azimuth angle has not been of main concern when discussing fuselage vibration level. It turns out to be correct as far as the major impedances are concerned.

The third conclusion is only a matter of course for those impedances whose source comes from the inertial loads. In the cases where the airloads have some of the major contributions, this conclusion is implicated in the blade motion in the following manner. The responses of an elastic blade could be quite different in hover and in forward flight. However, their responses having either ω or $\omega \pm \Omega$ frequencies (in rotating frame) are similar in the two flight conditions, thus resulting in similar impedance levels (within a range of several decibels) as far as the major impedances (having forcing frequency ω in body-fixed frame) are concerned.

Appendix: Derivation of Eqs. (15) and (16)

Substituting Eq. (14) into Eq. (13) and dividing by $e^{i\omega t}$, results in the following:

$$\sum_{k=-\infty}^{\infty} \sum_{n=-3}^{3} [-(\omega+k\Omega)^2 A_n + i(\omega+k\Omega) B_n + C_n] \hat{q}_k e^{i(n+k)\psi} = \sum_{m=-3}^{3} x_m e^{im\psi} \tag{A1}$$

where $i = \sqrt{-1}$.

Let the integer j be defined as:

$$j = n + k \tag{A2}$$

Eq. (A1) can then be arranged under the form

$$\sum_{j=-\infty}^{\infty} \sum_{k=j-3}^{j+3} R_{jk} \hat{q}_k e^{ij\psi} = \sum_{m=-3}^{3} x_m e^{im\psi} \tag{A3}$$

where R_{jk} is a matrix defined by Eq. (16). In order for this equation to hold for an arbitrary ψ, the following relation must hold for an arbitrary m:

$$\sum_{k=j-3}^{j+3} R_{jk} \hat{q}_k = x_j^* \qquad (-\infty < j < \infty) \tag{A4}$$

where

$$x_j^* = \begin{cases} x_j: \text{ if } -3 \le j \le 3 \\ 0: \text{ otherwise} \end{cases} \tag{A5}$$

To facilitate understanding, let us write down Eq. (A4) for $-5 \le j \le 5$ (see Fig. 8). A pair of integers (j, k) denotes the matrix R_{jk} defined by Eq. (16), while a blank denotes a zero matrix.

Now let us truncate the number k in Eq. (14) up to a finite integer h. For example, let us assume that $h=5$. This means

$$\hat{q}_k = 0 \qquad \text{for } |k| \ge 6 \tag{A6}$$

We can then construct a set of simultaneous equations to determine $\hat{q}_{-5}$ through $\hat{q}_5$; this set is enclosed by a broken line in Fig. 8.

A similar procedure can be applied for any integer h, and the general simultaneous equations for $\hat{q}_k$ ($|k| \le h$) can be easily shown to have the form of Eq. (15).

References

[1] Kato, K. and Yamane, T., "A Calculation of Rotor Impedance for Hovering, Articulated-Rotor Helicopters," *Journal of Aircraft*, Vol. 16, Jan. 1979, pp. 15-22.

[2] Peters, D. A., "Hingeless Rotor Frequency Response with Unsteady Inflow," NASA SP-352, 1974, pp. 1-12..

[3] Peters, D. A. and Ormiston, R. A., "Flapping Response Characteristics of Hingeless Rotor Blades by a Generalized Harmonic Balance Method," NASA TN D-7856, 1975.

[4] Miller, R. H., "Theoretical Determination of Rotor Blade Harmonic Airloads," MIT Tech. Rept. 107-2, Aug. 1964, p. 66.

[5] Hohenemser, K. H. and Yin, S-K., "Some Applications of the Method of Multiblade Coordinates," *Journal of the American Helicopter Society*, Vol. 17, July 1972, pp. 3-12.